A lesion of cortical area V2 selectively impairs the perception of the direction of first-order visual motion

Lucia M Vaina,[1,2] Sergei Soloviev,[1] Don C. Bienfang[3] and Alan Cowey[4]

[1]Brain and Vision Research Laboratory, Departments of Biomedical Engineering and Neurology, Boston University, 44 Cummington Street, Boston, MA 02215; [2]Departments of Neurology and Radiology and [3]Ophthalmology, Harvard Medical School, 75 Francis St, Boston, MA 02215, USA; [4]Department of Experimental Psychology, South Parks Road, Oxford OX1 3UD, UK

[1,CA]Corresponding Author

Received 18 January 2000; accepted 25 January 2000

Acknowledgements: We thank T.F. for his interest and participation in the experiments. The work was supported in part by NIH Grant EY07861 to L.M.V., by the Neurosensory Recovery Foundation grant to L.M.V., by MRC Grant G971398/B to A.C. and by a Network Travel Grant from the Oxford McDonnell-Pew Centre for Cognitive Neuroscience. We also thank Jose Diaz for programming the psychophysical stimuli.

Lesions of area MT/V5 in monkeys and its presumed homologue, the motion area, in humans impair motion perception, including the discrimination of the direction of global motion in random dot kinematograms. Here we report the results of similar tests on patient TF, who has a discrete and very small, unilateral infarct in the medial superior part of the right occipital cortex. Structural MRI, co-registered in software with a standardized human brain atlas, reveals that the lesion involves area V2. The patient was impaired in his retinotopically corresponding left lower quadrant on several motion tasks including discrimination in random dot kinematograms of direction, speed and motion-defined discontinuity. He was also impaired on tasks selectively involving first-order motion based on luminance contrast but not on second-order motion based on texture contrast. The results show that even though area MT/V5 is intact, motion perception is abnormal and, in particular, his perception of first-order motion is impaired. *NeuroReport* 11:1039–1044 © 2000 Lippincott Williams & Wilkins.

Key words: First- and second-order motion; Motion perception; V2; Visual cortex

INTRODUCTION

Although there is ample psychophysical evidence suggesting that distinct mechanisms are involved in processing first- and second-order visual motion (for recent reviews see [1,2]) recent neurophysiological studies revealed that neurons responding to both first- and second-order motion are ubiquitous in the visually responsive cortex. Cells in V1 [3], V2 the middle temporal area (MT) and its neighbors (e.g. MSTd) [4–6] and the inferior temporal lobe (IT) [7] of the macaque respond to both first- and second-order visual stimuli. Only a minority of cortical neurons, however, appear to respond to second-order motion which may account for the fact brain lesions appear to be more damaging to second-order than to first-order mechanisms [8–10]. There is only one example to date of a selective impairment of first-order motion, which is based on luminance contrast and not on texture contrast [11]. In this study the patient had a small medial lesion of one occipital lobe, tentatively localized to area V3 with possible involvement of the area V2. In the present investigation we report the results of similar tests on a patient whose unilateral lesion is even smaller and can be quite confidently localized to area V2 and which does not extend sufficiently into white matter to interrupt the projections from V1 to the motion area MT/V5.

THE PATIENT

Patient TF is a 60-year-old, right-handed, university-educated man who suffered a mild infarct involving part of his medial right occipital lobe, documented by CT without contrast. Neurological examination revealed no motor, language or cognitive deficits. The patient resumed full-time work a few weeks after the stroke. However, because he sensed his visual perception 6 weeks after the infarct to be abnormal he underwent a detailed neuro-ophthalmological examination. Visual acuity was normal (OD: 20/20 and OS; 20/30), as were intraocular pressures, pupillary response, eye movements, anterior segments, macula and retinal periphery in both eyes. There were no asymmetries in optokinetic nystagmus. However, both static and dynamic Goldmann perimetry revealed a left inferior homonymous quadrantanopia whose inner border

was from 20 to 30° away from the centre of the visual field, consistent with his occipital lobe lesion above the calcarine fissure. The entire neuro-ophthalmological examination was repeated 6 weeks later, by which time TF had full visual fields. However, he still reported some peculiarity of his vision in the former scotoma, namely that perception of motion in the left inferior quadrant was altered although static form and colour vision were normal. TF then expressed keen interest in exploring the nature of his selective perceptual deficits and gave informed consent according to the Boston University Human Subjects Committee and the Brigham and Women Hospital Human Subjects' Committee for psychophysical evaluation of his visual impairment and for obtaining a high resolution MRI scan of the brain. His performance on psychophysical tests of colour, form and spatial discrimination was normal. However, he was selectively impaired on most visual motion tasks for stimuli presented in the left inferior quadrant of his visual field.

In this study we first compare TF's ability to discriminate direction and speed of motion and to perceive direction or detect discontinuity in noisy motion stimuli. Second, we compare his direction discrimination ability in first- and second-order local and global motion displays. The rationale for selecting these particular tests is that TF's lesion is similar to that of the, until now, unique patient RA [11,12]. Like TF, RA was selectively impaired on a broad range of first-order motion tasks, but his performance was normal on all second-order motion tasks we employed. However, TF's lesion is significantly smaller and better localized to a particular part of the extrastriate visual cortex.

The lesion: MRI of the brain, without i.v. contrast, were obtained with a 1.5 T GE Signa System. Saggital T-1 weighted images, with 4 mm slices and 1 mm gap, and consecutive axial proton density regular spin echo images, with 3 mm slices and no gap, were obtained. An additional 124 coronal slices, 1.5 mm thick and no gap, were obtained by spoiled-gradient-echo acquisitions as described in detail in Vaina *et al*. [11]. Since TF's lesion was so small and mostly cortical it was appropriate to attempt to describe its location in a standardized anatomical framework. Accordingly, we performed a linear registration of the structural MRI data in Talairach space [13] by first using Medx neuroimaging software [14] to convert the individual slices into a 3D volume and then converting the raw imaging data into the conventional MINC format (Medical Image NetCDF). Subsequently we used the Montreal Neurological Institute Automated Linear Registration Package (MNI AutoReg) to transform points in the MRI space into Talairach space. The MNI AutoReg uses a completely automatic method based on multi-scale three-dimensional cross-correlation to register a given brain to the average MRI of 305 brains aligned with the Talaraich stereotaxic coordinate system [15]. An example of the visualisation of registered data for TF is shown in Fig. 1. The left column illustrates axial, saggital and coronal slices through the infarct, the middle column shows corresponding slices from the reference average brain used for registration, and the right column shows the superimposition of the respective slices. TF's lesion is unusually small, but could be followed across four consecutive slices; $x = 11–13$, $y = -67$ to -73, and $z = 18–24$.

Anatomically (with the aid of the Talairach Daemon software http://ric.uthscsa.edu/projects/talairachdaemon.html) the Talairach coordinates of the lesion correspond to a small medial region in the right occipital lobe, centered in the cuneus and Brodmann area 18, and lying just above the calcarine fissure in what is almost certainly V2 but perhaps slightly encroaching on V3.

PSYCHOPHYSICAL METHODS AND RESULTS

Apparatus and procedures: The apparatus and psychophysical procedures are only briefly summarized here. Details are provided in Vaina *et al*. [3,4]. The displays were generated and the responses collected and analysed using a PowerMac computer. The stimuli were presented in the centre of a colour monitor (Apple Trinitron 0.25 mm pitch; 13 inch; 640×480 pixels; viewing area 235×176 mm; vertical scanning frequency 66.7 Hz and P22 phosphor, 256 grey levels). Each motion display was generated by a rapid sequence of static frames. In all conditions, each test-frame lasted 45 ms and stimuli were displayed for 22 frames (1 s). In all the tests employed the stimulus speed was 3 deg/s. Except where stated otherwise, dot density was 2 dots/deg^2, the mean luminance of the stimulus area was $\sim$0.51 cd/m^2 and of the background 0.23 cd/m^2. The difficulty of the tests was titrated by an adaptive staircase procedure described in Vaina *et al*. [10] which was used to determine each subject's threshold, computed as the arithmetic mean of the last six reversals. The y axis of each of the data graphs in Fig. 2 and Fig. 3 indicates for each test the specific parameter whose values were varied using the adaptive staircase procedure.

Testing took place in a dark room, in which the only illumination came from the computer monitor. After 5 min dark adaptation, subjects received practice trials of varying difficulty which ensured that they understood the task. Between trials subjects viewed the uniform blank screen, except for the dark fixation mark. Throughout the trial and testing periods subjects sat 60 cm from the screen and binocularly fixated a small black mark to the left or right of the imaginary border of the stimulus aperture and positioned such that the stimulus was presented at 2° eccentricity to the left or right inferior quadrant of the visual field, just below the horizontal meridian. Subjects responded verbally and the examiner entered the response via the computer keyboard. In Fig. 2 and Fig. 3 filled circles show the data from stimuli presented in the right lower visual quadrant (RIQ) and unfilled circles show the results for stimuli presented in the lower left visual quadrant (LIQ).

Direction discrimination: The display was a sparse random dot kinematogram in a circular aperture 10° in diameter. All the dots moved upwards but at a variable angle to the left or right of true vertical (Fig. 2a), indicated by a vertical line 0.5° above the display. In a 2AFC procedure subjects were asked whether the dots moved to the right or the left with respect to the vertical line. Figure 2b shows that in his right lower quadrant, TF's threshold was similar to that of four age-matched control subjects,

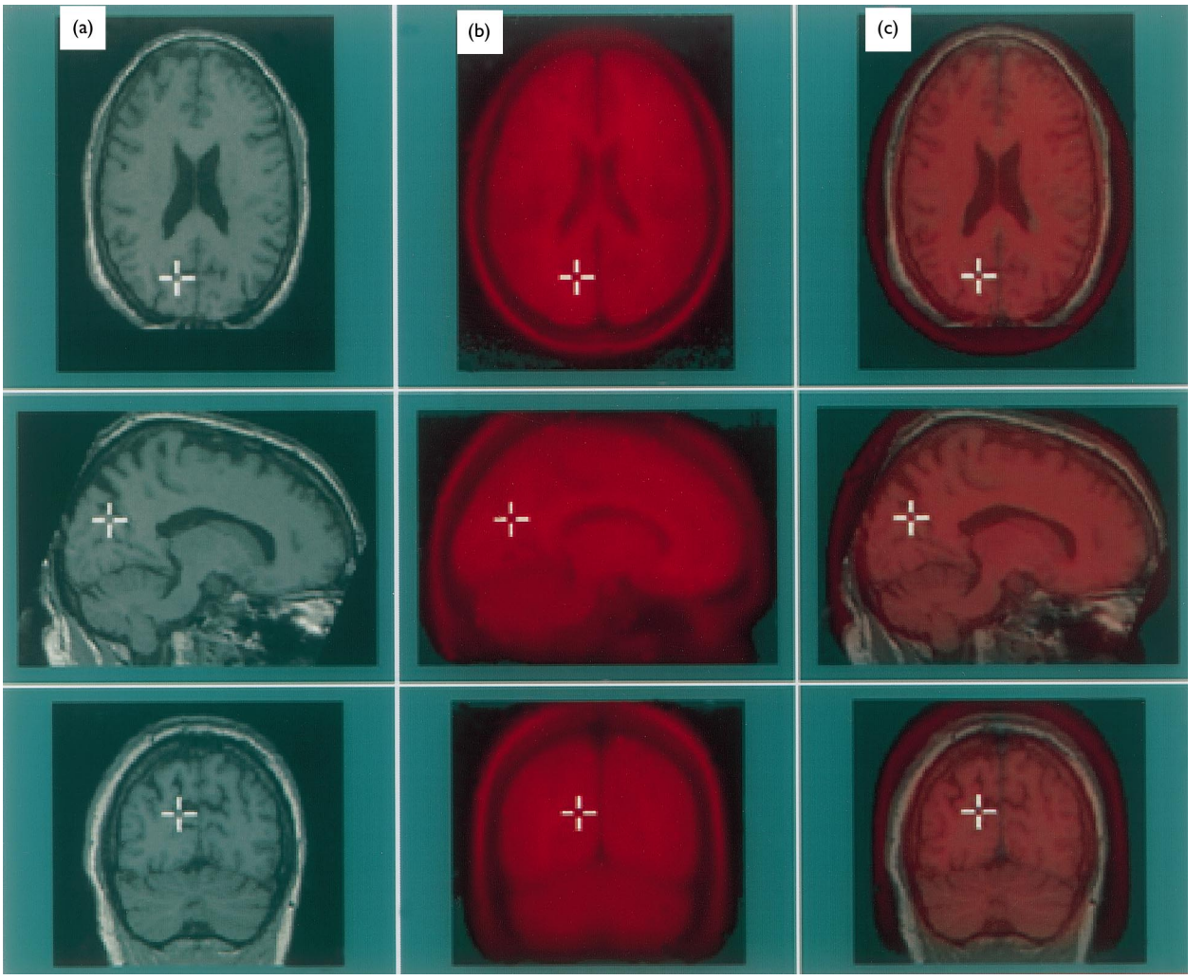

Fig. 1. The registration in Talairach coordinates of the brain lesion in patient TF. (**a**) Slices of TF's brain through the centre of the lesion in axial, saggital and coronal planes. (**b**) Corresponding slices from the MNI average brain (prepared from 305 different brains). (**c**) The patient's brain superimposed on the average brain. The size of the lesion, ρ, determined by $\rho = \sqrt{\Delta x^2 + \Delta y^2 + \Delta z^2}$, where Δx, Δy, Δz are its length in three dimensions, is $\rho = 11.2$ mm.

but in his left lower quadrant there was a roughly four-fold increase in threshold.

Speed discrimination: Random dot kinematograms were presented in two circular apertures, each 10° in diameter, one displayed 500 ms after the other (Fig. 2c). In each trial, the dots within each aperture moved at the same speed in random directions but at a different speed in the two intervals. The standard speed of 3 deg/sec, presented in one or other aperture at random, varied randomly from trial to trial by $\pm 20\%$ to deter subjects from trying to judge speed by distance travelled. The speed in the other aperture was titrated downwards, starting at 6 deg/s. Fig. 2d shows that TF's speed discrimination threshold was doubled in his left lower quadrant in comparison with seven age-matched control subjects but was tripled in comparison to his threshold in his intact right lower quadrant, where he performed better than the majority of the control subjects.

Motion coherence: The stimuli (Fig. 2e) were stochastic random dot kinematograms with a coherent motion direction signal of variable strength (signal dots) embedded in masking motion noise (noise dots), presented in a 10° diameter circular aperture. In a 4AFC tasks subjects were asked to determine whether the global motion of the display was to the left, right, up or down. Figure 2f shows that in his impaired left lower quadrant TF's coherence threshold was more than three times greater than in his right lower quadrant, where his performance was no different from that of five age-matched control subjects.

Motion discontinuity: The stimulus was similar to the previous one (motion coherence) except that in half of the trials the display appeared bisected by an illusory line of variable orientation (as shown in Fig. 2g). Within each semicircle the direction of the coherent motion was either upward or downward, and it was opposite to that in the other semicircle thus giving the vivid impression of a

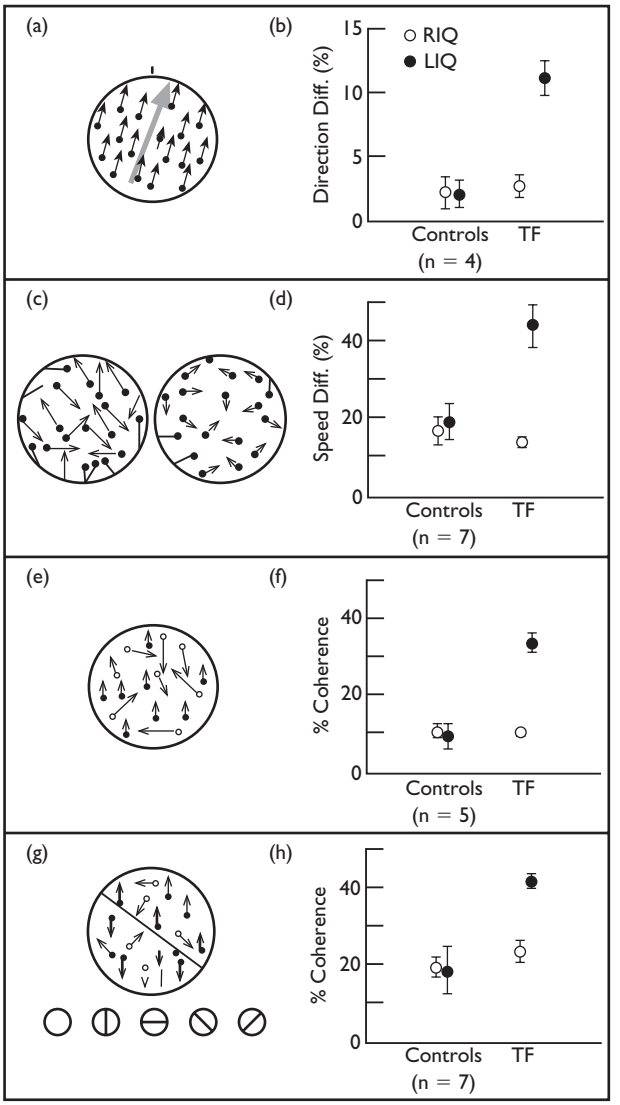

Fig. 2. The figures on the left represent schematically the stimuli used in the following tests: A: direction discrimination; C: speed discrimination; E: motion coherence and G: motion discontinuity. On the right are the results for each test from age matched normal control subjects and TF. The open circles represent the results for stimuli presented in the right inferior quadrant, and filled circles the results for stimuli shown in the left inferior quadrant. Note that TF was selectively impaired on all these tests for stimuli presented in the left inferior quadrant corresponding to his right medial occipital lesion.

bisecting line. The subjects had to indicate whether the moving display was homogeneous or not. Using the adaptive staircase procedure on the level of coherence, the test automatically calculated the threshold of proportion of signal dots necessary for subjects' discrimination between homogeneous motion and presence of a discontinuity. Figure 2h shows that in his impaired lower left quadrant TF's threshold was about double that in his right quadrant or in either quadrant of seven control subjects.

D-max in first- and second-order motion: D-max, or maximum displacement, corresponds to the maximum jump between frames that allows subjects to perceive the

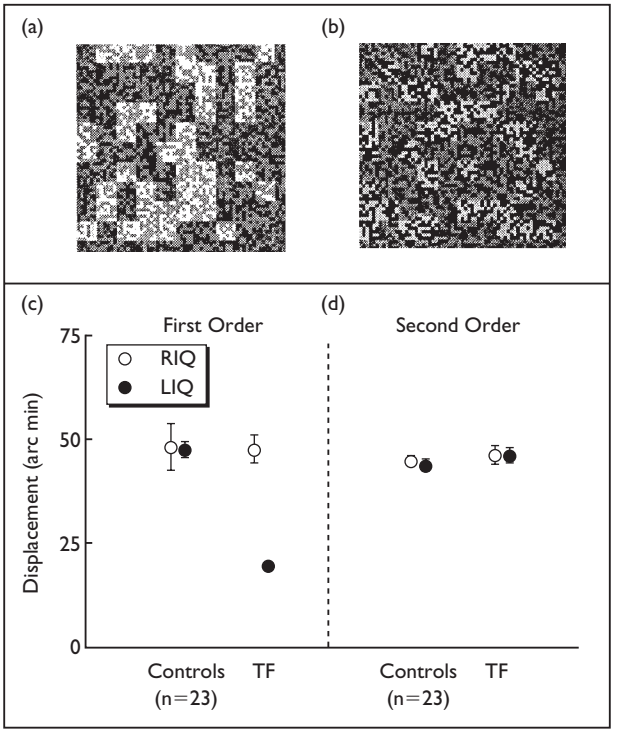

Fig. 3. Schematic of the display used to measure direction discrimination in textured random dot kinematograms. In (**a**) the motion is first-order: a group of micropatterns differing from the background in luminance is shifted coherently to the left or to the right. In (**b**) the motion is second-order: the shifting micropatterns differ from the background in contrast but in mean luminance. (**c**,**d**) Performance of TF and control subjects on the two tasks for stimuli presented in the inferior quadrants. TF was impaired in his left visual quadrant for the first-order stimulus but not for the second-order stimulus.

leftward or rightward direction of the stimulus (textured pattern). The display subtended 10×10 deg arc, and was divided into a notional grid of 38×38 blocks, each consisting of a dense random dot microtexture (Fig. 3a,b). The dots defining the microtextures were evenly distributed on or off, as represented by different gray levels. Because the random reassignment of the on and off state of a dot in the background and tokens the whole stimulus appeared to flicker. On each trial 42% of the blocks, randomly assigned and called token-blocks, moved left or right while the remaining 58% constituted the background. The mean luminance of the background was $9.5\,cd/m^2$ with mean contrast of 0.2.

Depending on the luminance and contrast ratios between the blocks and the background there were two test conditions: (1) first-order motion (Fig. 3a), in which a block differed from the background in mean luminance (12.3 *vs* $9.5\,cd/m^2$) but not mean contrast (which was kept at constant 0.2); (2) second-order motion (Fig. 3b), in which a block differed from the background in mean contrast (0.6 *vs* 0.2) but not mean luminance. The motion display consisted of two successive 45 ms frames with zero inter-frame interval and the spatial pattern of texture defining the tokens and the background varied randomly from frame-to-frame. The size of the step of the displacement

was varied from trial to trial using the adaptive staircase procedure.

Figure 3c shows that for the first-order motion stimulus in the right lower quadrant TF's D-max was little different from that of the two control subjects, whereas in his impaired lower left quadrant his D-max was more than halved. His performance, however, was normal in both left and right inferior quadrants for second-order motion stimuli (Fig. 3d).

Direction discrimination in first- and second-order global motion: The display, shown in Fig. 4a,b, was like that used to measure D-max but the strength of the motion signal was systematically varied by changing the proportion of token-blocks that moved in the same direction, left or right. The remaining moving blocks appeared from frame to frame at random locations, creating the impression of random textured flicker. Moving block density was 2 blocks/deg^2 and speed was 3 deg/s. The mean luminance of first-order blocks was 12.3 cd m^2 and contrast was 0.2, while the mean luminance of second-order blocks was 9.5 cd m^2 and contrast was 0.6. The stimulus was presented for twelve 45 ms frames, with zero interframe interval. Figure 4c,d shows that although TF was not impaired on the second-order motion stimulus, his threshold for discriminating the direction of first-order global motion was increased by 4-fold in his left lower quadrant compared to his performance in the right inferior quadrant and the performance of the 17 normal control subjects.

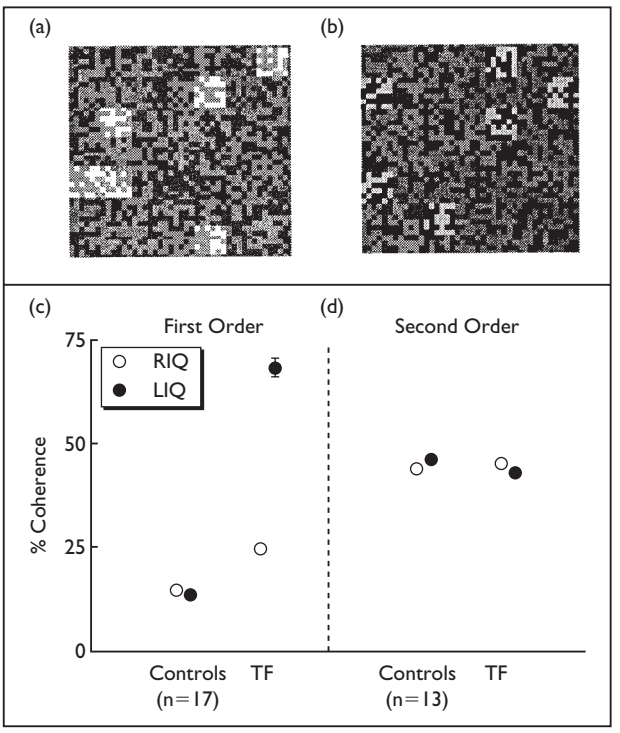

Fig. 4. On the top are shown schematic views of the first-order motion coherence task (**a**) and the second-order motion coherence task (**b**). On the bottom, (**c**) and (**d**) show the threshold coherence necessary to reliably perform these tasks from control subjects and TF. Note that compared to the normal controls, TF's performance on the first-order task was impaired for stimulus presentation in his left inferior quadrant.

DISCUSSION

We found that TF, a patient with a small (about 11 mm) infarct in the medial superior occipital lobe, could not process first-order motion normally in his left lower visual quadrant. The result confirms our earlier findings [11] in a patient with a larger lesion. By co-registering the structural MR images and a standardized brain (using the Montreal Neurological Institute atlas) and determining the co-ordinates of the lesion in Talairach space it was possible to localize the lesion, perhaps exclusively, to upper V2, corresponding to the left lower visual quadrant. It was argued by Horton and Hoyt [16] that quadrantic field defects whose horizontal border respects the horizontal retinal meridian, as in patient TF before his quadrantanopia resolved, probably reflect damage to V2, which is respectively divided above and below V1 into an upper and lower representation of the two contralateral retinal quadrants. However, the two patients studied by Horton and Hoyt had long-lasting and dense quadrantic field defects that reached or almost reached the fovea whereas TF's scotoma was restricted to eccentricities well beyond the macula and rapidly resolved. The likely explanation for the difference is that in TF there was no or only short-lasting damage to adjacent V1, as also indicated by the MR images.

From the lesion analysis it appears that the direct projection from V1 to MT suggested to provide the neural circuitry for the early cortical stages of first-order motion [17] was normal in TF, while the projection from V1 to MT via V2, assumed to mediate the second-order motion pathway [17] was disrupted. This model is inconsistent with the psychophsyical data presented here which showed that TF's performance was impaired on some first-order motion tasks but normal on second-order motion. While the classical models of early diverging parallel pathways selectively mediating these two types of motion cannot explain TF's data, they can be accounted for by the recent model of Clifford and Vaina [1]. In this model a first-order channel computes motion at coarse and fine scales, and a second-order motion channel operates at the coarse scale. In the context of this model, TF's performance may be viewed as disabling the fine scale of first-order motion processing which results in his impairment on discrimination of direction, speed and motion-defined discontinuity. However, the operating coarse channel would explain his normal performance on the second-order stimuli and the fact that he is not blind to the other motion tasks reported here. Could the coarse motion channel be mediated by the pathway V1–dV3–MT [18]? A recent fMRI study in normal human subjects [19] shows that the cortical areas V3, VP and MT elicit the strongest responses to second-order motion, and these areas were not involved in TF's lesion, thus providing an anatomical basis for his normal second-order motion perception and for the hypothesis that TF's motion perception is mediated by the coarse channel of Clifford and Vaina's model [1].

CONCLUSION

A patient with unilateral damage to the upper part of cortical area V2, corresponding to his left lower visual quadrant, was impaired at discriminating the direction of motion in noisy first-order random dot displays. As his

performance was normal for similar displays involving second-order motion the result supports the idea of regional specialization in motion processing in extrastriate visual areas.

REFERENCES

1. Clifford C and Vaina L. *Vis Res* **39**, 113–130 (1999).
2. Baker CLJ. *Curr Opin Neurobiol* **9**, 461–466 (1999).
3. Chaudhuri A and Albright T. *Vis Neurosci* **14**, 949–962 (1997).
4. Albright TD. *Science* **255**, 1141–1143 (1992).
5. O'Keefe LP and Movshon JA. *Vis Neurosci* **15**, 305–317 (1998).
6. Geesaman BJ and Andersen RA. *J Neurosci* **16**, 4716–4732 (1996).
7. Sáry G, Vogels R, Kovács G and Orban GA. *J Neurophysiol* **73**, 1341–1354 (1995).
8. Plant GT and Nakayama K. *Brain* **116**, 1337–1353 (1993).
9. Greenlee MW and Smith AT. *J Neurosci* **17**, 804–818 (1997).
10. Vaina L and Cowey A. *Proc R Soc Lond B* **263**, 1225–1232 (1996).
11. Vaina LM, Makris N, Kennedy D and Cowey A. *Vis Neurosci* **15**, 333–348 (1998).
12. Vaina L, Cowey A and Kennedy D. *Hum Brain Mapp* **7**, 67–77 (1999).
13. Talairach J and Tournoux P. *Co-Planar Stereotaxic Atlas of the Human Brain*. New York: Thieme Medical Publishers, 1988.
14. Sensor Systems Inc. Sterling, VA (1999).
15. Collins DL, Neelin P, Peters TM and Evans AC. *J Comp Assist Tomogr* **18**, 192–205 (1994).
16. Horton J and Hoyt W. *Brain* **114**, 1703–1718 (1991).
17. Wilson HR, Ferrera VP and Yo C. *Vis Neurosci* **9**, 79–97 (1992).
18. Boussaoud D, Ungerleider LG and Desimone R. *J Comp Neurol* **296**, 462–495 (1990).
19. Smith AT, Greenlee MW, Singh KD *et al. J Neurosci* **18**, 3816–3830 (1998).